Analytical and Bioanalytical Chemistry (2019) 411:4327–4338
https://doi.org/10.1007/s00216-019-01665-w

TRENDS

Polydopamine: surface coating, molecular imprinting, and electrochemistry—successful applications and future perspectives in (bio)analysis

Pasquale Palladino[1] · Francesca Bettazzi[1] · Simona Scarano[1]

Received: 7 December 2018 / Revised: 25 January 2019 / Accepted: 31 January 2019 / Published online: 26 February 2019

Abstract

Dopamine oxidation and self-polymerization have recently attracted great interest arising from the versatile chemistry of this endogenous catecholamine. Particularly interesting are the applications of polydopamine for surface coating, molecular imprinting, and electrochemistry, which are reviewed here, covering the broad fields of medicine, materials science, and (bio)analytical chemistry. Nonetheless, the peculiar physicochemical properties of dopamine and polydopamine, due to the redox potential of the catechol moiety, are not fully exploited. We have confidence in increasing the applications of dopamine through a large variety of research approaches, including the use of naturally occurring or synthetic dopamine analogues and copolymers. Accordingly, our efforts in this direction are focused on proposing a role for polydopamine in quantitative applications, evaluating analytical performance, cost, reproducibility, and versatility of the methods developed, and also revisiting standard (bio)analytical platforms.

Keywords Polydopamine · Molecularly imprinted polymers · Surface coating · Electrochemistry · Bioanalysis

Introduction

The huge importance of endogenous dopamine (DA) for the human renal, hormonal, and central nervous systems and the consequent severe clinical conditions associated with DA concentration anomalies, including schizophrenia and Parkinson's disease, have generated more than 200,000 scientific articles over the past 80 years. A more recent and intriguing outcome from this plethora of information is represented by DA oxidation and self-polymerization [1–3]. The electrochemical and chemical reaction pathway for polydopamine (PDA) formation in aqueous solutions requires the synthesis of 5,6-indolequinone from DA [1, 4, 5]. Notably, the polymer growth is inhibited by low pH (below 4) and high concentration of various electrolytes that impair the preliminary intramolecular cyclization of oxidized DA by decreasing nitrogen nucleophilicity [1]. Since the pioneering investigations and application of DA polymerization by electrodeposition [1, 2], and then by O_2/pH-induced oxidation [3], thousands of articles concerning PDA synthesis, study, and application have been published. Notably, the last 4 years accounts for almost 80% of all the scientific production, underlining the increased interest arising from the versatile chemistry of this endogenous catecholamine and its complex polymerization mechanism [6–9]. The reactivity of DA and PDA is associated with the redox potential of the catechol moiety, which has been exploited to produce optically and catalytically active metal nanoparticles in situ [10–12]. This feature, which is responsible for the cross-linking of DA, can be enhanced by chemical oxidants [13–15], UV irradiation [16], or microwave irradiation [17], influencing the coating of PDA at the nanometer scale used for a variety of physical, chemical, and biological studies [7, 8]. However, this research field is still young and challenging for application of PDA-coated surfaces in medicine, the energy sector, and industrial manufacturing, for example [7, 8]. In particular, a promising field of PDA research is surface coating for molecular sensing and affinity separation for pharmaceutical studies and clinical applications [18, 19] because of the peculiar physicochemical properties of

Published in the topical collection *Young Investigators in (Bio-)Analytical Chemistry* with guest editors Erin Baker, Kerstin Leopold, Francesco Ricci, and Wei Wang.

✉ Simona Scarano
simona.scarano@unifi.it

[1] Department of Chemistry 'Ugo Schiff', University of Florence, via della Lastruccia 3–13, 50019 Sesto Fiorentino, FI, Italy

PDA, including photoreactivity, thermoreactivity, electroreactivity, and chemical reactivity [10–12], and the molecular immobilization and imprinting capability of this biopolymer [2, 20–23]. Here we survey this demanding area of bioanalytical research, focusing on the state of the art of PDA applications for coating, imprinting, and electrochemistry, and offering a long-term vision of the use of this polymer to its full potential.

PDA imprinting

The preparation of molecularly imprinted polymers (MIPs) requires noncovalent interactions or the formation of reversible covalent adducts between a molecular template of interest and a functional monomer(s) before the polymerization of the latter. Subsequent template removal generates synthetic binding sites within the polymer with high selectivity and sensitivity for the template molecule [24–27]. In this framework, DA appears particularly suitable for molecular imprinting because of its hydrophilicity, biocompatibility, self-assembly, and universal coating capability [3, 7]. In particular, the simple DA–analyte copolymerization and the subsequent analyte removal have been used to generate a robust and biocompatible nanometer film for quantitative analysis of molecules without an additional self-assembled sublayer. Here we review selected publications of use to categorize the research lines for PDA application in MIPs based on substrate geometry and composition or on the template size (Fig. 1 and Table 1).

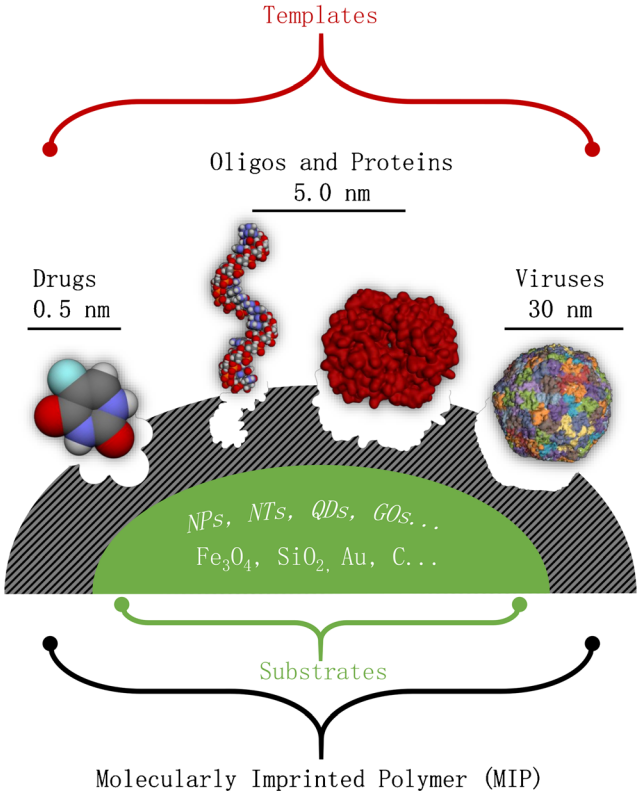

Fig. 1 Polydopamine imprinting on substrates with several kinds of geometries and composition. Dopamine–template copolymerization and the subsequent template removal generates synthetic binding sites within the polymer with a broad range of dimensions. GOs graphite oxide sheets, NPs nanoparticles, NTs nanotubes, QDs quantum dots

MIP substrates: geometry and composition

Among the variety of PDA layer applications [18, 19, 21], PDA adhesion for molecular imprinting is essentially associated with solid-phase extraction and microextraction. Most of these functional nanocomposites are nanoparticles and materials with similar geometry such as carbon dots, quantum dots, and polystyrene microbeads. Less abundant are the studies involving the PDA coating and imprinting on nanotubes, graphite oxide (GO), macroscopic surfaces (gold and quartz), and hydrogels. Commonly, deposition and imprinting have been studied by scanning electron microscopy, transmission electron microscopy, dynamic light scattering, and atomic force microscopy (AFM) before and after the polymer adhesion to determine the morphological features (i.e., shape, size distribution, and dispersibility of nanocomposites and topography of extended surfaces).

MIP on nanoparticles

The size of the imprinted particles is dependent on the synthetic protocol and may differ by some orders of magnitudes, resulting in huge differences between the preparations in terms of the amount of PDA per nanoparticle and, more generally, the surface-to-volume ratio and the properties of the nanocomposites. In detail, magnetic MIPs are built with a core of Fe_3O_4 [28–35], which can contain additional shells (e.g., SiO_2, carbon dots, Nafion®) contributing to the global structural and physical features of magnetic MIPs [32- 35]. However, the outer shell of PDA constituting the MIP is independent of the substrate size and composition, appearing tunable in a thickness range of 5–100 nm for a single growth step [28, 29, 31, 33]. For example, very small fluorescent carbon dots with a magnetic Fe_3O_4 core (mean diameter around 12 nm) have been coated with a shell of PDA of about 25 nm [32]. Nevertheless, much larger particles (up to 1 μm) still preserve an outer shell of PDA with similar size [30, 34,3 5].

MIP on nanotubes

Porous tubular structures at the nanometer scale have been reported in the form of carbon nanotubes, multiwalled carbon nanotubes, and halloysite nanotubes [36–40]. Their magnetic counterparts are obtained by the grafting

Table 1 Polydopamine molecularly imprinted polymer: substrate features and analytes

Substrate		Analyte		
Geometry	Composition	Name	Application	Reference
Nanoparticles	Fe_3O_4	Gallic acid	Separation	[28]
		Lysozyme	Separation	[29]
		Amino acids	Separation	[30]
		Metabolites	Separation	[31]
		5-Fluorouracil	Drug delivery	[46]
		Albumin	Separation	[52]
		Hepatitis A virus	Detection	[53]
	Fe_3O_4/carbon dots	Hemoglobin	Detection	[32]
	Fe_3O_4/SiO_2	Gallic acid	Separation	[33]
		Hemoglobin	Separation	[34]
	Fe_3O_4/Nafion®	Diethylstilbestrol	Separation	[35]
	SiO_2	Bacteriophages	Detection	[23]
		Hepatitis A Virus	Detection	[54]
Nanotubes	Carbon nanotubes/Fe_3O_4	Lysozyme	Separation	[36]
	Multiwalled carbon nanotubes	Vanillin	Detection	[37]
		Sunset yellow	Detection	[38]
	Multiwalled carbon nanotubes/Fe_3O_4	Cinnamic acid	Separation	[39]
	Halloysite nanotubes	Albumin	Separation	[40]
Flat surfaces	Graphite oxide/Fe_3O_4	Albumin	Separation	[41]
	Graphite oxide	Hemoglobin	Separation	[42]
	Gold chips	Troponin T	Detection	[20]
		IgG	Detection	[43]
		Sulfamethoxazole	Detection	[44]
	Quartz crystals	Domoic acid	Detection	[45]
Nanowires	Alumina oxide	Hemoglobin	Separation	[47]
Microbeads	Polystyrene/quantum dots	IgG	Detection	[48]
Microhollows	Pickering hydrogels	Hemoglobin	Separation	[49]
			Separation	[50]
Amorphous	Mesoporous carbon/Fe_3O_4	Bromelain	Separation	[51]

of Fe_3O_4 nanoparticles onto nanotubes [36, 39]. The outer diameter of the nanotubes is variable, but is in the range of a few tens of nanometers [36–40]. The PDA-coating shell before and after the template imprinting procedure ranges between a few nanometers [36–38, 40] and 40 nm [39]. Notably, a thinner MIP in comparison with a nonimprinted polymer (NIP) has been ascribed to DA polymerization inhibition by the template [38], whereas morphology changes for an MIP on analyte binding have not been reported. Halloysite nanotubes are very peculiar because of their chemically reactive hollow tubular structure, which can assume a negatively charged silica layer on the outer surface and a positively charged alumina layer on the inner surface. Although successfully imprinted, the coating layer appears to be not uniform, likely because of the redox properties of the surface of halloysite nanotubes [40].

MIP on flat surfaces

Two-dimensional imprinting has been achieved by PDA adhesion on molecular (e.g., GO) or extended (e.g., Au/SiO_2) flat surfaces. In detail, sheets of GO have been commonly synthesized from graphite and then coated with PDA, thus producing a larger surface-to-volume ratio and a higher number of binding sites per unit volume in comparison with nanoparticles [41]. Nevertheless, Fe_3O_4 nanoparticles can also be deposited on GO sheets before imprinting to confer magnetic properties to these substrates [41]. Electron microscopy images show a curved surface for these nanocomposites before and after imprinting [41, 42]. Furthermore, morphology analysis (AFM, scanning electron microscopy) of the two-dimensional molecularly imprinted materials allows observation of the thickness of both the GO sheets (approximately 1 nm) and the PDA adhesion layer (a few nanometers) [42].

There are no observable differences between the MIP and the NIP because the size of the template and, consequently, the dimensions of the binding site are below the limit of resolution of the microscopy techniques. On the other hand, this morphology conservation of nanocomposites on imprinting, template removal, and template rebinding confirms the stability of the PDA layer. Moreover, it provides indirect proof that the greater binding capacity of the MIP in comparison with the NIP is due to the effective molecular imprinting and not to PDA nonspecific assembly modification. Regarding the extended deposition and imprinting of PDA, gold chips or SiO_2 bare crystals have been used as substrates for molecular detection and analysis by surface plasmon resonance [20, 43], electrochemical [44], and quartz crystal microbalance [45] techniques. On the basis of theoretical design, the PDA thickness has been tuned between a few nanometers and a few tens of nanometers to obtain the best template orientation during the molecular imprinting. This results in the most analyte-accessible functional cavities in the polymer layer [43]. The surface morphology of bare substrates, NIP and MIP, has usually been investigated by AFM [44, 45], measuring the film thickness, roughness, and homogeneity after coating, imprinting, and washing stages, leading to a topographic characterization of PDA deposition and imprinting [44].

MIP template size: mesoscopically imprinted polymers

The first example reported in the literature involved a PDA-based MIP for the capacitive sensing of nicotine [2]. Later, PDA was used as a recognition element for much larger targets, such as proteins or viruses. Therefore, it appears reasonable that several new applications of PDA-based MIPs will be related to the imprinting and sensing of living cells and viruses in biological and environmental samples. This expansion of applicability to larger and much more complex analytes has been possible because of the self-assembly of DA in aqueous media that generates a biocompatible and highly hydrophilic polymer. PDA-unique features have easily overcome the problem associated with poor stability of biological molecules in organic solvents previously required for solubilization and reaction of other kinds of functional monomers and cross-linking agents. Consequently, "mesoscopically imprinted polymers" appears to be a more suitable and more comprehensive name for the current and future developments of biopolymer imprinting strategies in bioanalysis.

Small-molecule imprinting

To the best of our knowledge, nicotine was the first molecule imprinted in PDA for molecular detection [2], anticipating plentiful applications in MIP sensor development, mostly by use of nanoparticles as the substrate. In particular, the imprinting of small molecules (molecular mass ranging between 0.1 and 1 kDa) has involved amino acids [30], sugars [31], estrogens [35], flavorings [37], colorants [38], phenolic acids [39], antibiotics [44], toxins [45], and chemotherapeutic agents in cancer [46]. Notably, it has been reported that the release of an anticancer molecule imprinted on PDA-coated Fe_3O_4 nanoparticles increases in the presence of a magnetic field, resulting in effective control of tumor growth in animal models [46], thus paving the way for future studies and applications of MIPs on magnetic substrates.

Oligonucleotide, enzyme, and immunoglobulin imprinting

After an early report on human-hemoglobin-imprinted PDA showing high rebinding capacity and specific recognition in aqueous media [47], several PDA-imprinted substrates were developed for rapid and specific recognition of proteins and oligonucleotides with potential application to separation of analytes from real and complex matrices [21, 48–51]. The adsorption selectivity and binding specificity were evaluated. The imprinting factor expresses the ratio between the MIP and the NIP absorption capability toward the template, and the selectivity coefficient evaluates unspecific binding of the MIP and competitive analytes of a similar shape, size, and isoelectric point. For example, studies on bovine serum albumin imprinting and separation from blood samples have given imprinting factors between 1.7 and 6.2 and selectivity coefficients between 1.3 and 4.5 [40, 41, 52]. Similar studies have been reported for different oligonucleotides, enzymes, and immunoglobulins with a molecular mass ranging from 7 to 150 kDa up to a few tens of nanometers in length [21].

Virus imprinting

Very recently, trace amounts of several viruses have been directly and specifically detected by use of virus-imprinted PDA; namely, hepatitis A virus (HAV) and bacteriophages (f2, T4, P1, and M13) [23, 53, 54]. In the case of HAV, sensing has been achieved also in human serum by use of virus-imprinted SiO_2@PDA, or magnetic Fe_3O_4@PDA, nanoparticles with a low limit of detection of approximately 10^{-11} M and an imprinting factor of around 2 [53, 54]. Remarkably, electron microscopy images of modified nanoparticles show surface protuberances between the PDA imprinting and washing stages, and hollows after template removal, with a size and shape compatible with the HAV units (30 nm in diameter), providing direct evidence of virus imprinting. In the case of the bacteriophages mentioned earlier, it was shown that the virus morphology severely affects the PDA imprinting on silica particles. Consequently, the binding selectivity and kinetics decrease with size increase from the smallest and spherical phage f2 (approximately 26 nm in diameter) to the largest and elongated phage M13 (900 nm) [23]. However, the study

authors recognize that the apparent negative correlation between dimensions and imprinting requires further investigations to exclude other factors (e.g., the influence of specific capsid proteins of the viruses investigated) [23].

Electrochemical and photoelectrochemical characterization and use of PDA films in (bio) analysis

Because of their intrinsic characteristics of being potentially fast, easy, and low cost, electrochemical and photoelectrochemical techniques are widely used for the development of bioassays for the detection of analytes of clinical interest, such as clinical biomarkers [55, 56]. However, electrode surface modification strategies are often challenging because bioanalytical applications require highly biocompatible and properly functionalized surfaces to bind the biorecognition material and retain its biological activity. Moreover, the binding should be sufficiently strong to avoid the leaching of the biomaterial from the sensor surface [57]. The increasing need for easy, efficient, and versatile immobilization methods in bioanalytical assays led to the investigation of the potential applications of PDA in electrochemistry (Table 2).

Deposition of a PDA layer on an electrode: chemical oxidation versus electrodeposition

The fundamental mechanism for the formation of PDA is still not fully understood [58, 59]. In most of the applications, the polymerization of DA is achieved by the chemical process reported by Lee et al. [3]. Briefly, a combination of bulk and surface polymerization is induced at a basic pH. Simple immersion of substrates in a dilute aqueous solution of DA, buffered at typical marine environment pH [10 mM tris(hydroxymethyl)aminomethane, pH 8.5], results in spontaneous deposition of a thin adherent polymeric film. Polymerization involves the oxidation of catechol to quinone, which further reacts with amine and the other catechols and quinones, leading to the formation of the polymeric film. Despite the film not being chemically homogeneous, the coating obtained with this straightforward procedure shows great reactivity toward amine and thiol groups [57, 60, 61]. Such

Table 2 Polydopamine (PDA): deposition strategy, electrode features, applications, and methods

Polymerization	PDA-modified electrode	Analyte	Methods	Reference
Chemical	GCE	Laccase and glucose oxidase	CV and chronoamperometry	[57]
	Silicon wafers/amorphous carbon	PDA	CV and EIS	[60]
	Laccase@Au on pyrolytic graphite	Norepinephrine and microRNA	CV and EIS	[63]
	WS_2/ITO	5-Hydroxymethylcytosine	Photocurrent and EIS	[79]
	AgNPs@graphene on GCE	Adenine and guanine	DPV	[64]
	AuNPs/myoglobin/graphene on GCE	H_2O_2	CV and amperometry	[65]
	AuNPs/ITO/graphene quantum dots	H_2O_2	CV and amperometry	[66]
	Fe_3O4 nanoparticles/thionine on GCE	H_2O_2	CV and amperometry	[69]
	Gold electrode	Sulfate-reducing bacteria	EIS	[68]
	Gold electrode	PDA	CV in the presence of $Fe(CN)_6^{3-}$	[73]
	PDA/WO_3/ITO	CYFRA 21-1	Photocurrent and EIS	[80]
	TiO_2 nanotube arrays	H_2O_2	Photocurrent and EIS	[82]
	ITO/WO_3/CdS/carbon nanotubes	Insulin	Photocurrent and EIS	[84]
	Si/SiO_2	PDA	Photocurrent and CV	[87]
	La-doped CdS/3D $ZnIn_2S_4$/Au@ZnO on ITO	NT-proBNP	Photocurrent	[88]
Electrochemical	GCE	pH sensing	CV	[58]
	GCE	Dopamine	CV	[59]
	Electroplated gold on cleaned gold	H_2O_2 and uric acid	CV and amperometry	[62]
	Gold surfaces	DNA	CV	[67]
	Gold electrode	Dopamine	CV	[70]
	GCE	Dopamine	CV and SWV	[71]
	Screen-printed carbon electrode	Guanine	CV, chronoamperometry, and EIS	[72]

AgNP silver nanoparticle, *AuNP* gold nanoparticle, *CV* cyclic voltammetry, *EIS* electrochemical impedance spectroscopy, *DPV* differential pulse voltammetry, *GCE* glassy carbon electrode, *ITO* indium tin oxide, *NT-proBNP* N-terminal prohormone of brain natriuretic peptide, *SWV* square wave voltammetry

coatings, often called "pseudomelanin," can be easily modified by a single-step reaction leading to several kinds of modified surfaces, including surfaces decorated with metal nanoparticles [62, 63], such as silver nanoparticles [64] or gold nanoparticles (AuNPs) [65, 66], via the reduction from solution of the corresponding cations. This reduction step is possible because of the presence of the catechol groups, which undergo oxidation at the quinone functional groups during the reduction of the metallic cations. The reactivity of quinone groups in PDA films toward primary amines and thiols can be advantageously used for covalent binding of target biomolecules, through a Schiff base formation or Michael-type addition, for sensor development [6, 57, 67–69].

A possible drawback of this method is the difficulty in controlling the localization and the surface morphology of the deposited PDA film. Despite this polymerization strategy being easily reproducible and universally established for a wide range of materials [67], an alternative method for the preparation of PDA can be achieved by an electrochemical polymerization process. Since the electropolymerization occurs at the interface of the electrode, PDA films can be generated in a highly controlled and spatially selective manner. The mechanism of PDA electropolymerization has been deeply investigated since the late 1960s, when Hawley et al. [4] proposed essentially two electrochemical mechanisms related to DA oxidation; namely, the so-called ECC and ECE mechanisms (where "E" and "C" denote the electrochemical step and the chemical step, respectively). The oxidation of DA is considered to finally lead to melanin-like polymers and thus the whole process is complex. In the ECE mechanism, the polymerization goes through three steps: In the first step, the formation of *o*-dopaminoquinone occurs after exchange of two electrons and two protons. It is commonly known that quinones are quite reactive and can undergo nucleophilic coupling. Depending on the experimental conditions used, mechanisms with more complicated sequences of electrochemical and chemical steps were also proposed [67, 70]. Dopaminoquinone contains both an electron-deficient ring and an electron-donor amine group. As the result of a 1,4 Michael addition and on deprotonation of the amine group, a cyclization reaction can occur. Therefore, in the second step, *o*-dopaminoquinone undergoes intramolecular cyclization, which leads to leucodopaminochrome, which is easily oxidized in the third step to dopaminochrome, which may be transformed into melanin polymers.

Voltammetric studies of DA have further elucidated the oxidation steps leading to PDA formation [71, 72]. In detail, during consecutive scans, a continuous decrease of the peak current intensities, due to the formation of PDA layers (Fig. 2a, b), has been reported. This effect demonstrates that the electrode surface is affected by the fouling of the electrode caused by the PDA layers as PDA grows with successive scans up to complete electrode fouling. Nevertheless, two redox peaks are still present and can be attributed to the oxidation and reduction of the catechol and quinone units present in PDA [58, 73]. Furthermore, for DA in solution, the anodic peak current is linearly proportional to the square root of the scan rate, as usual for an electrode transfer reaction controlled by both adsorption and diffusion [71], whereas for PDA film adsorbed on the electrode, the linearity of the anodic and cathodic peak currents versus scan rate indicates a surface-confined voltammetry corresponding to a "thin layer" type [72], as typical of electrode-adsorbed species [74]. The oxidation peak potential moves to lower values with increasing solution pH, indicating the involvement of protons in the electrochemical reaction [72]. These features were used in the fabrication of a pH sensor based on glassy carbon electrodes and PDA films [58].

It clearly appears that the accurate assignment of all the redox processes occurring on PDA films is a challenging task [57]. The easy and universal application of PDA and the wide variety of uses in (bio)analytical assay development is in contrast with the complex electrochemical behavior. Moreover, this is also in contrast with the well-established redox processes of common conducting polymers, such as polypyrrole, polythiophene, and polyaniline [75–78].

Photoelectrochemical properties of PDA and photoelectrochemical bioassays

Photoelectrochemical sensors are powerful and reliable tools for bioanalysis because of their inherent operational simplicity, low background current, and high detection sensitivity [79–81]. Recently, photoelectrochemistry has been applied to the detection of several analytes, such as H_2O_2 [82], nucleic acids [83], proteins [84], and glucose [85].

The effectiveness of the photoelectrochemical assay mainly relies on the performance of the photoactive material. Recent studies demonstrated that quinones can be successfully used in energy applications through the hybridization of these of molecules with several kinds of materials [86, 87]. In this framework, some recent reports demonstrated that the synthesized PDA exhibited semiconducting properties and a special charge transfer capability because of the presence of the π–π system. The presence of a highest occupied molecular orbital and a lowest unoccupied molecular orbital makes PDA a useful photosensitizer to promote the absorption of visible light, increasing light harvesting efficiency and charge collection efficiency in photoelectrochemical bioassays (Fig. 2c) and offering interesting opportunities for the development of high-performance optoelectronic devices [87, 88].

Outlook

The intriguing versatility of PDA has led to its relevant role in several research fields, first of all in the science of

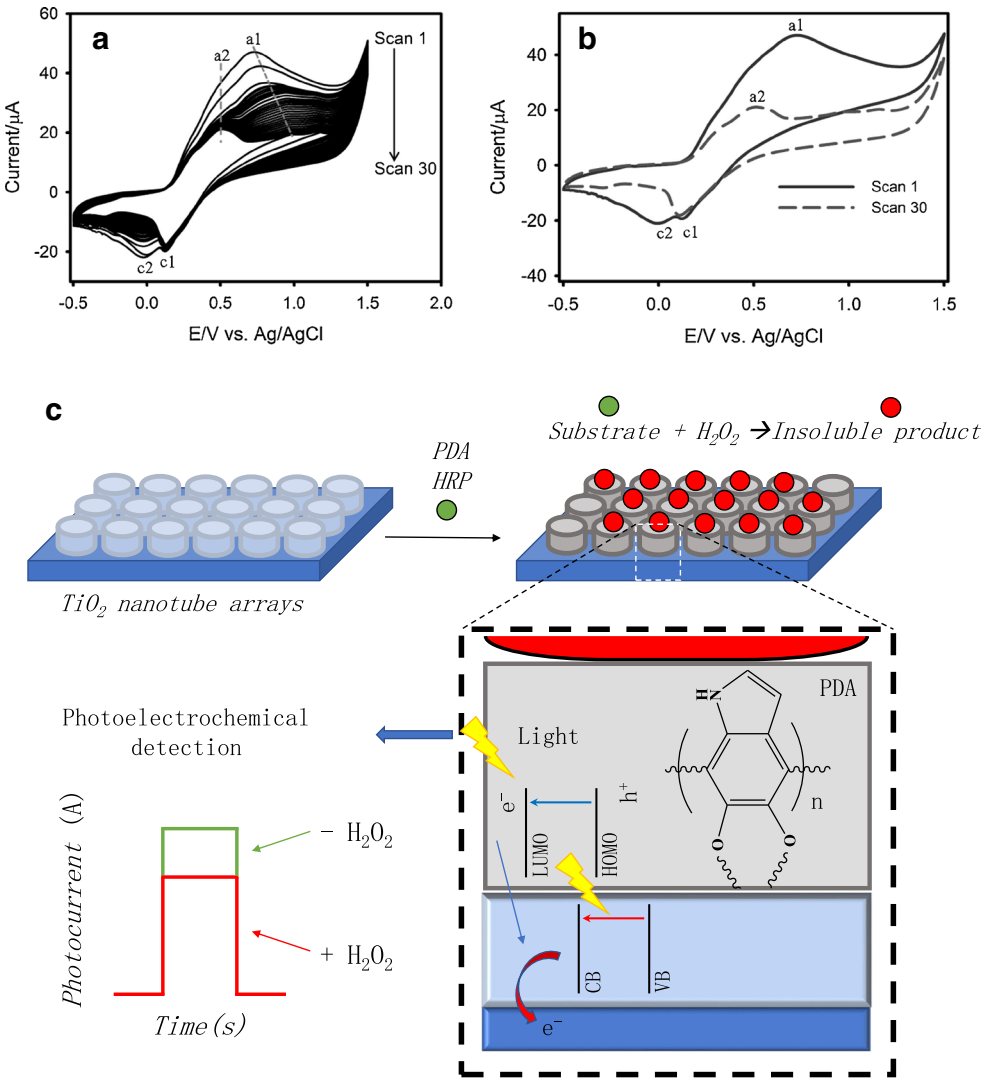

Fig. 2 **a**, **b** Polydopamine (PDA) electropolymerization by cyclic voltammetry at a screen-printed carbon electrode (5.0 mM dopamine, pH 7.0, 100 mV s^{-1}). **c** Mechanism of photoinduced charge separation caused by PDA. PDA-assisted decoration of TiO_2 nanotube arrays with horseradish peroxidase (HRP) and subsequent photocurrent decrease in the presence of H_2O_2 due to the formation of insoluble enzymatic product. CB conduction band, HOMO highest occupied molecular orbital, LUMO lowest unoccupied molecular orbital, VB valence band. (**a**, **b** Reprinted with permission from [72]; **c** redrawn with permission from [82])

biocompatible materials for drug delivery and cancer therapy. Undoubtedly, the autoassembly and coating abilities of this polymer are the most exploited features in such applications. Functional surface moieties (quinones/catechols and amines) add further possibilities in the subsequent (bio)chemical modification of PDA coatings, expanding their role beyond expectations. However, at present the lack of innovative uses of PDA in the field of (bio)analytical chemistry is surprising, excluding those mentioned earlier for the synthesis of MIPs and, in general, for electrochemical-based applications. In this framework, original and unexplored ways of investigating the possible use of DA/PDA with direct impact in quantitative (bio)analytics are sought. One of the poorly investigated aspects of DA polymerization to produce PDA films is the kinetics of formation of these layers at the surface of the material considered. For example, during the formation of the PDA adhesive layer on a polystyrene surface (e.g., disposable laboratory equipment such as microtiter plates, UV–vis cuvettes, tips), the polymerization step may be perturbed in significant ways to obtain analytical information useful for macromolecules (e.g., protein detection in complex matrices) [9].

In particular, the co-presence in solution of proteins directly limits the thickness of the final PDA layer adhered on the substrate [9]. This approach, considered until now a drawback in MIP production for protein detection, deserves further investigation. The broad absorption band of PDA in the visible range permits investigation of the optical response at almost any wavelength, and with low-cost and widely used plate readers commonly used in immune-based assays (i.e., ELISA). The prospective application of such a bioanalytical method would open new and crucial scenarios in light of the serious failing of current methods for quantification of total protein in biological fluids (Fig. 3, panel a). In this regard, application to nanoplasmonic-based detection of low molecular weight analytes was recently reported. In particular, our group has explored the possibility of developing "plasmonic cuvettes" by in situ growth of controlled AuNPs by PDA for localized surface plasmon resonance (LSPR)-based

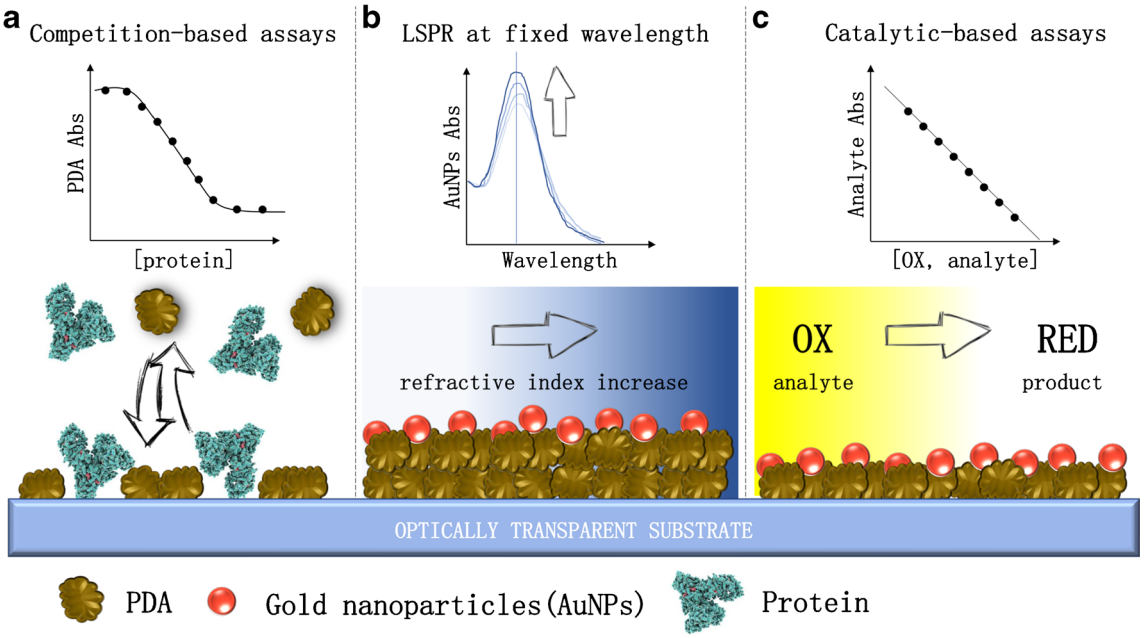

Fig. 3 Innovative uses of polydopamine (PDA) in the field of (bio)analytical chemistry: competition-based assay for quantification of total protein in biological fluids (**a**), localized surface plasmon resonance (LSPR)-based quantitative assay at fixed wavelength for applications in clinical, food, and environmental control (**b**), and catalytic-based assay for redox reactions (**c**). Abs absorbance, OX oxidized, RED reduced

quantitative assays at a fixed wavelength using a conventional spectrophotometer [11]. This research starts from the consideration of the role of PDA films decorated with metal nanoparticles. Despite the presence of numerous articles dealing with the in situ reduction of metal ions at the PDA surface to obtain nanoparticles, no indication of the rationale behind the process has been provided; we recently obtained some results in that direction, both by modulating the PDA formation protocol [11] before exposure of PDA to Au(III) and by varying the metal ion concentration, leaving fixed the PDA film features [12]. In the first case, we clarified the crucial role played by PDA morphology in producing different populations of AuNPs, providing different plasmonic behaviors. The surprising evidence is that not only the reducing power of PDA toward Au(III) increases linearly with thickness but also that the plasmonic behavior of AuNPs changes accordingly. Considering the increasing demand for low-cost protocols to modulate different LSPR regimes for bioanalytical applications [89, 90], this result stimulated further investigation. Deposited nanostructures with different features (size, geometry, density, etc.) generally exhibit a hybrid behavior between pure wavelength sensitivity at constant extinction and pure absorbance sensitivity at constant wavelength. The significant result is that PDA thickness can modulate the plasmonic response from the classical wavelength shift to the absorbance change (Fig. 3, panel b). This approach was applied to the quantitative determination of fermentable sugars in beer wort, with excellent analytical performance compared with refractometers used routinely in cellars. Moreover, the easy reading of the "photonic" UV–vis cuvettes at fixed wavelength with portable spectrometers allows one to suggest further applications in clinical, food, and environmental control. PDA-based nanocomposites for quantitative assays based on the catalytic activity of metal nanoparticles may represent a further easy and low-cost approach for colorimetric determination of (bio)analytical targets in human specimens [12]. In other words, with greater understanding of PDA behavior, novel analytical applications can be developed by combining PDA redox characteristics and kinetics of film formation.

By the reverse approach, once the PDA film type is fixed, the role of different metal ion concentrations in producing different AuNP populations also deserves further investigation. In this context, PDA films decorated with in situ grown AuNPs (AuNPs@PDA) were tested for their catalytic activity toward nitrophenol isomers. As widely reported in the literature, AuNPs (in solution or supported) act as efficient catalysts in a large variety of organic reduction and oxidation reactions. But, until now, the reduction of nitrophenols and in particular of *p*-nitrophenol has been reported mainly as case studies to characterize and compare different catalytic substrates, whereas for quantitative determination, high-performance liquid chromatography alone or combined with mass spectrometry with the use of radiolabels generally remains the technique of choice. In a recent study, the in-plate, fast, low-cost, and high-throughput determination of *p*-nitrophenol on AuNPs@PDA substrates in aqueous solution and in urine was achieved, providing new information on the behavior of these nanocomposites during the catalytic process. Different AuNP populations may show different catalytic ability and chemical resistance on the basis of the preparation protocol [in terms of Au(III)

concentration] used. Only a specific concentration range of Au(III) guarantees AuNPs@PDA resistant to the reduction process, whereas outside this range, complete dissolution of the nanocomposite occurs. The result is easily obtained with a routinely used ELISA reader at 415 nm, where the absorbance decrease of the *p*-nitrophenolate ion (the optically active species generated by *p*-nitrophenol with excess of $NaBH_4$) provides quantitative and linearly correlated information on the *p*-nitrophenol present in the sample (Fig. 3, panel c). In conclusion, recent advancements with regard to PDA decorated with metallic nanoparticles widen the possibilities in this emerging field. Several metallic precursors are reducible at the PDA surface, giving nanoparticles with different and exciting optical, catalytic, and functional properties.

As a whole, PDA is very promising tool not only in the already explored fields of applied medicine and materials science but also in (bio)analytical chemistry. Our efforts in this direction are focused on proposing a role for this polymer in quantitative applications, evaluating analytical performance, cost, reproducibility, and versatility of the methods developed and also revisiting standard platforms, such as ELISA readers, portable spectrophotometers, and electrochemical devices. The reactivity of DA to give PDA in different environmental conditions remains only partially explored, and we have concrete indications in several directions to increase its use through a large variety of strategies, also involving DA homologues and other suitable copolymers playing different roles in this extremely fast changing research field.

Acknowledgements The authors thank the Ministry of Education, University and Research (MIUR) for financial support through the scientific program SIR2014 Scientific Independence of Young Researchers (RBSI1455LK), Horizon 2020, European Union funding for research and innovation, and Regione Toscana for the scientific program Plasmonic Biosensor Analysis of Nucleic Acid Biomarkers (PLABAN; D53D16002290009).

Compliance with ethical standards

Conflict of interest The authors declare that they have no competing interests.

References

1. Li Y, Liu M, Xiang C, Xie Q, Yao S. Electrochemical quartz crystal microbalance study on growth and property of the polymer deposit at gold electrodes during oxidation of dopamine in aqueous solutions. Thin Solid Films. 2006;497(1–2):270–8. https://doi.org/10.1016/j.tsf.2005.10.048.
2. Liu K, Wei WZ, Zeng JX, Liu XY, Gao YP. Application of a novel electrosynthesized polydopamine-imprinted film to the capacitive sensing of nicotine. Anal Bioanal Chem. 2006;385(4):724–9. https://doi.org/10.1007/s00216-006-0489-z.
3. Lee H, Dellatore SM, Miller WM, Messersmith PB. Mussel-inspired surface chemistry for multifunctional coatings. Science. 2007;318(5849):426–30. https://doi.org/10.1126/science.1147241.
4. Hawley MD, Tatawawadi SV, Piekarski S, Adams RN. Electrochemical studies of the oxidation pathways of catecholamines. J Am Chem Soc. 1967;89(2):447–50. https://doi.org/10.1021/ja00978a051.
5. Saraji M, Bagheri A. Electropolymerization of indole and study of electrochemical behavior of the polymer in aqueous solutions. Synth Met. 1998;98(1):57–63. https://doi.org/10.1016/S0379-6779(98)00151-9.
6. Yang J, Stuart MAC, Kamperman M. Jack of all trades: versatile catechol crosslinking mechanisms. Chem Soc Rev. 2014;43(24):8271–98. https://doi.org/10.1039/c4cs00185k.
7. Ryu JH, Messersmith PB, Lee H. Polydopamine surface chemistry: a decade of discovery. ACS Appl Mater Interfaces. 2018;10(9):7523–40. https://doi.org/10.1021/acsami.7b19865.
8. Qiu WZ, Yang HC, Xu ZK. Dopamine-assisted co-deposition: An emerging and promising strategy for surface modification. Adv Colloid Interf Sci. 2018;256:111–25. https://doi.org/10.1016/j.cis.2018.04.011.
9. Palladino P, Brittoli A, Pascale E, Minunni M, Scarano S. Colorimetric determination of total protein content in serum based on the polydopamine/protein adsorption competition on microplates. Talanta. 2019;198:15–22. https://doi.org/10.1016/j.talanta.2019.01.095.
10. Wang JG, Hua X, Li M, Long YT. Mussel-inspired polydopamine functionalized plasmonic nanocomposites for single-particle catalysis. ACS Appl Mater Interfaces. 2017;9(3):3016–23. https://doi.org/10.1021/acsami.6b14689.
11. Scarano S, Pascale E, Palladino P, Fratini E, Minunni M. Determination of fermentable sugars in beer wort by gold nanoparticles@polydopamine: a layer-by-layer approach for localized surface plasmon resonance measurements at fixed wavelength. Talanta. 2018;183:24–32. https://doi.org/10.1016/j.talanta.2018.02.044.
12. Scarano S, Palladino P, Pascale E, Brittoli A, Minunni M. Colorimetric determination of p-nitrophenol on ELISA microwells modified with an adhesive polydopamine nanofilm containing catalytically active gold nanoparticles. Microchim Acta. 2019;186(3):146. https://doi.org/10.1007/s00604-019-3259-2.
13. Wei Q, Zhang F, Li J, Li B, Zhao C. Oxidant-induced dopamine polymerization for multifunctional coatings. Polym Chem. 2010;1:1430–3. https://doi.org/10.1039/c0py00215a.
14. Hong SH, Hong S, Ryou MH, Choi JW, Kang SM, Lee H. Sprayable ultrafast polydopamine surface modifications. Adv Mater Interfaces. 2016;3:1500857. https://doi.org/10.1002/admi.201500857.
15. Ponzio F, Barthès J, Bour J, Michel M, Bertani P, Hemmerlé J, et al. Oxidant control of polydopamine surface chemistry in acids: a mechanism-based entry to superhydrophilic-superoleophobic coatings. Chem Mater. 2016;28:4697–705. https://doi.org/10.1021/acs.chemmater.6b01587.
16. Du X, Li L, Li J, Yang C, Frenkel N, Welle A, et al. UV-triggered dopamine polymerization: control of polymerization, surface coating, and photopatterning. Adv Mater. 2014;26:8029–33. https://doi.org/10.1002/adma.201403709.
17. Lee M, Lee SH, Oh IK, Lee H. Microwave-accelerated rapid, chemical oxidant-free, material-independent surface chemistry of poly(dopamine). Small. 2017;13:1600443. https://doi.org/10.1002/smll.201600443.
18. Li H, Jia Y, Peng H, Li J. Recent developments in dopamine-based materials for cancer diagnosis and therapy. Adv Colloid Interf Sci. 2018;252:1–20. https://doi.org/10.1016/j.cis.2018.01.001.

19. Barclay TG, Hegab HM, Clarke SR, Ginic-Markovic M. Versatile surface modification using polydopamine and related polycatecholamines: chemistry, structure, and applications. Adv Mater Interfaces. 2017;4(19):1601192. https://doi.org/10.1002/admi.201601192.
20. Palladino P, Minunni M, Scarano S. Cardiac Troponin T capture and detection in real-time via epitope-imprinted polymer and optical biosensing. Biosens Bioelectron. 2018;106:93–8. https://doi.org/10.1016/j.bios.2018.01.068.
21. Che D, Cheng J, Ji Z, Zhang S, Li G, Sun Z, et al. Recent advances and applications of polydopamine-derived adsorbents for sample pretreatment. Trends Anal Chem. 2017;97:1–14. https://doi.org/10.1016/j.trac.2017.08.002.
22. Chen D, Mei Y, Hu W, Li CM. Electrochemically enhanced antibody immobilization on polydopamine thin film for sensitive surface plasmon resonance immunoassay. Talanta. 2018;182:470–5. https://doi.org/10.1016/j.talanta.2018.02.038.
23. Li N, Liu YJ, Liu F, Luo MF, Wan YC, Huang Z, et al. Bio-inspired virus imprinted polymer for prevention of viral infections. Acta Biomater. 2017;51:175–83. https://doi.org/10.1016/j.actbio.2017.01.017.
24. Wulff G. Molecular recognition in polymers prepared by imprinting with templates. In: Ford WE (ed) Polymeric reagents and catalysis. ACS symposium series 308, Washington: American Chemical Society; 1986. p. 186–230. https://doi.org/10.1021/bk-1986-0308.ch009.
25. Zamora-Galvez A, Morales-Narváez E, Mayorga-Martinez CC, Merkoçi A. Nanomaterials connected to antibodies and molecularly imprinted polymers as bio/receptors for bio/sensor applications. Appl Mater Today. 2017;9:387–401. https://doi.org/10.1016/j.apmt.2017.09.006.
26. Dabrowski M, Lach P, Cieplak M, Kutner W. Nanostructured molecularly imprinted polymers for protein chemosensing. Biosens Bioelectron. 2017;102:17–26. https://doi.org/10.1016/j.bios.2017.10.045.
27. Gui R, Jin H, Guo H, Wang Z. Recent advances and future prospects in molecularly imprinted polymers-based electrochemical biosensors. Biosens Bioelectron. 2018;100:56–70. https://doi.org/10.1016/j.bios.2017.08.058.
28. Zhang J, Li B, Yue H, Wang J, Zheng Y. Highly selective and efficient imprinted polymers based on carboxyl-functionalized magnetic nanoparticles for the extraction of gallic acid from pomegranate rind. J Sep Sci. 2018;41(2):540–7. https://doi.org/10.1002/jssc.201700822.
29. Zhang M, Zhang X, He X, Chen L, Zhang Y. A self-assembled polydopamine film on the surface of magnetic nanoparticles for specific capture of protein. Nanoscale. 2012;4(10):3141–7. https://doi.org/10.1039/c2nr30316g.
30. Wang XN, Liang RP, Meng XY, Qiu JD. One-step synthesis of mussel-inspired molecularly imprinted magnetic polymer as stationary phase for chip-based open tubular capillary electrochromatography enantioseparation. J Chromatogr A. 2014;1362:301–8. https://doi.org/10.1016/j.chroma.2014.08.044.
31. Zhang YZ, Zhang JW, Wang CZ, Zhou LD, Zhang QH, Yuan CS. Polydopamine-coated magnetic molecularly imprinted polymers with fragment template for identification of Pulsatilla saponin metabolites in rat feces with UPLC-Q-TOF-MS. J Agric Food Chem. 2018;66(3):653–60. https://doi.org/10.1021/acs.jafc.7b05747.
32. Lv P, Xie D, Zhang Z. Magnetic carbon dots based molecularly imprinted polymers for fluorescent detection of bovine hemoglobin. Talanta. 2018;188:145–51. https://doi.org/10.1016/j.talanta.2018.05.068.
33. Hu X, Xie L, Guo J, Li H, Jiang X, Zhang Y, et al. Hydrophilic gallic acid–imprinted polymers over magnetic mesoporous silica microspheres with excellent molecular recognition ability in aqueous fruit juices. Food Chem. 2015;179:206–12. https://doi.org/10.1016/j.foodchem.2015.02.007.
34. Jia X, Xu M, Wang Y, Ran D, Yang S, Zhang M. Polydopamine-based molecular imprinting on silica-modified magnetic nanoparticles for recognition and separation of bovine hemoglobin. Analyst. 2013;138(2):651–8. https://doi.org/10.1039/c2an36313e.
35. Qiao L, Gan N, Hu F, Wang D, Lan H, Li T, et al. Magnetic nanospheres with a molecularly imprinted shell for the preconcentration of diethylstilbestrol. Microchim Acta. 2014;181(11–12):1341–51. https://doi.org/10.1007/s00604-014-1257-y.
36. Gao R, Zhang L, Hao Y, Cui X, Liu D, Zhang M, et al. Novel polydopamine imprinting layers coated magnetic carbon nanotubes for specific separation of lysozyme from egg white. Talanta. 2015;144:1125–32. https://doi.org/10.1016/j.talanta.2015.07.090.
37. Wu W, Yang L, Zhao F, Zeng B. A vanillin electrochemical sensor based on molecularly imprinted poly (1-vinyl-3-octylimidazole hexafluoride phosphorus)−multi-walled carbon nanotubes@polydopamine–carboxyl single-walled carbon nanotubes composite. Sensors Actuators B Chem. 2017;239:481–7. https://doi.org/10.1016/j.snb.2016.08.041.
38. Yin ZZ, Cheng SW, Xu LB, Liu HY, Huang K, Li L, et al. Highly sensitive and selective sensor for sunset yellow based on molecularly imprinted polydopamine-coated multi-walled carbon nanotubes. Biosens Bioelectron. 2018;100:565–70. https://doi.org/10.1016/j.bios.2017.10.010.
39. Yin Y, Yan L, Zhang Z, Wang J, Luo N. Polydopamine-coated magnetic molecularly imprinted polymer for the selective solid-phase extraction of cinnamic acid, ferulic acid and caffeic acid from radix scrophulariae sample. J Sep Sci. 2016;39(8):1480–8. https://doi.org/10.1002/jssc.201600026.
40. Zhu X, Li H, Liu H, Peng W, Zhong S, Wang Y. Halloysite-based dopamine-imprinted polymer for selective protein capture. J Sep Sci. 2016;39(12):2431–7. https://doi.org/10.1002/jssc.201600168.
41. Chen F, Zhao W, Zhang J, Kong J. Magnetic two-dimensional molecularly imprinted materials for the recognition and separation of proteins. Phys Chem Chem Phys. 2016;18(2):718–25. https://doi.org/10.1039/c5cp04218f.
42. Luo J, Jiang S, Liu X. Efficient one-pot synthesis of mussel-inspired molecularly imprinted polymer coated graphene for protein-specific recognition and fast separation. J Phys Chem C. 2013;117(36):18448–56. https://doi.org/10.1021/jp405171w.
43. Tretjakov A, Syritski V, Reut J, Boroznjak R, Volobujeva O, Öpik A. Surface molecularly imprinted polydopamine films for recognition of immunoglobulin G. Microchim Acta. 2013;180(15–16):1433–42. https://doi.org/10.1007/s00604-013-1039-y.
44. Turco A, Corvaglia S, Mazzotta E, Pompa PP, Malitesta C. Preparation and characterization of molecularly imprinted mussel inspired film as antifouling and selective layer for electrochemical detection of sulfamethoxazole. Sensors Actuators B Chem. 2018;255:3374–83. https://doi.org/10.1016/j.snb.2017.09.164.
45. Zhou WH, Tang SF, Yao QH, Chen FR, Yang HH, Wang XR. A quartz crystal microbalance sensor based on mussel-inspired molecularly imprinted polymer. Biosens Bioelectron. 2010;26(2):585–9. https://doi.org/10.1016/j.bios.2010.07.024.
46. Hashemi-Moghaddam H, Kazemi-Bagsangani S, Jamili M, Zavareh S. Evaluation of magnetic nanoparticles coated by 5-fluorouracil imprinted polymer for controlled drug delivery in mouse breast cancer model. Int J Pharm. 2016;497(1–2):228–38. https://doi.org/10.1016/j.ijpharm.2015.11.040.
47. Ouyang R, Lei J, Ju H. Surface molecularly imprinted nanowire for protein specific recognition. Chem Commun. 2008;44:5761–3. https://doi.org/10.1039/b810248a.
48. Liu Y, Liu L, He Y, He Q, Ma H. Quantum-dots-encoded-microbeads based molecularly imprinted polymer. Biosens Bioelectron. 2016;77:886–93. https://doi.org/10.1016/j.bios.2015.10.024.

49. Sun Y, Li Y, Xu J, Huang L, Qiu T, Zhong S. Interconnectivity of macroporous molecularly imprinted polymers fabricated by hydroxyapatite-stabilized Pickering high internal phase emulsions-hydrogels for the selective recognition of protein. Colloids Surf B. 2017;155:142–9. https://doi.org/10.1016/j.colsurfb.2017.04.009.
50. Sun Y, Zhong S. Nanoscale trifunctional bovine hemoglobin for fabricating molecularly imprinted polydopamine via Pickering emulsions-hydrogels polymerization. Colloids Surf B. 2017;159:131–8. https://doi.org/10.1016/j.colsurfb.2017.07.069.
51. Xu X, Liu R, Guo P, Luo Z, Cai X, Shu H, et al. Fabrication of a novel magnetic mesoporous molecularly imprinted polymer based on pericarpium granati-derived carrier for selective absorption of bromelain. Food Chem. 2018;256:91–7. https://doi.org/10.1016/j.foodchem.2018.02.118.
52. Gao R, Zhang L, Hao Y, Cui X, Tang Y. Specific removal of protein using protein imprinted polydopamine shells on modified amino-functionalized magnetic nanoparticles. RSC Adv. 2014;4(110):64514–24. https://doi.org/10.1039/c4ra07965e.
53. Zhang F, Luo L, Gong H, Chen C, Cai C. A magnetic molecularly imprinted optical chemical sensor for specific recognition of trace quantities of virus. RSC Adv. 2018;8(56):3226228. https://doi.org/10.1039/c8ra06204h.
54. Yang B, Gong H, Chen C, Chen X, Cai C. A virus resonance light scattering sensor based on mussel-inspired molecularly imprinted polymers for high sensitive and high selective detection of hepatitis A virus. Biosens Bioelectron. 2017;87:679–85. https://doi.org/10.1016/j.bios.2016.08.087.
55. Voccia D, Bettazzi F, Baydemir G, Palchetti I. Alkaline-phosphatase-based nanostructure assemblies for electrochemical detection of microRNAs. J Nanosci Nanotechnol. 2015;15(5):3378–84. https://doi.org/10.1166/jnn.2015.10201.
56. Baydemir G, Bettazzi F, Palchetti I, Voccia D. Strategies for the development of an electrochemical bioassay for TNF-alpha detection by using a non-immunoglobulin bioreceptor. Talanta. 2016;141:141–7. https://doi.org/10.1016/j.talanta.2016.01.021.
57. Almeida LC, Correia JP, Viana AS. Electrochemical and optical characterization of thin polydopamine films on carbon surfaces for enzymatic sensors. Electrochim Acta. 2018;263:480–9. https://doi.org/10.1016/j.electacta.2018.01.077.
58. Amiri M, Amali E, Nematollahzadeh A, Salehniya H. Polydopamine films: voltammetric sensor for pH monitoring. Sensors Actuators B Chem. 2016;228:53–8. https://doi.org/10.1016/j.snb.2016.01.012.
59. Ismail I, Okajima T, Kawauchi S, Ohsaka T. Studies on the early oxidation process of dopamine by electrochemical measurements and quantum chemical calculations. Electrochim Acta. 2016;211:777–86. https://doi.org/10.1016/j.electacta.2016.05.056.
60. Ball V, Del Frari D, Toniazzo V, Ruch D. Kinetics of polydopamine film deposition as a function of pH and dopamine concentration: Insights in the polydopamine deposition mechanism. J Colloid Interface Sci. 2012;386(1):366–72. https://doi.org/10.1016/j.jcis.2012.07.030.
61. Lee H, Rho J, Messersmith PB. Facile conjugation of biomolecules onto surfaces via mussel adhesive protein inspired, coatings. Adv Mater. 2009;21(4):431–4. https://doi.org/10.1002/adma.200801222.
62. Dai M, Huang T, Chao L, Xie Q, Tan Y, Chen C, et al. Horseradish peroxidase-catalyzed polymerization of l-DOPA for mono-/bi-enzyme immobilization and amperometric biosensing of H_2O_2 and uric acid. Talanta. 2016;149:117–23. https://doi.org/10.1016/j.talanta.2015.11.047.
63. Chen T, Xu Y, Wei S, Li A, Huang L, Liu J. A signal amplification system constructed by bi-enzymes and bi-nanospheres for sensitive detection of norepinephrine and miRNA. Biosens Bioelectron. 2019;124–125:224–32. https://doi.org/10.1016/j.bios.2018.10.030.
64. Huang KJ, Wang L, Wang HB, Gan T, Wu YY, Li J, et al. Electrochemical biosensor based on silver nanoparticles-polydopamine- graphene nanocomposite for sensitive determination of adenine and guanine. Talanta. 2013;114:43–8. https://doi.org/10.1016/j.talanta.2013.04.017.
65. Liu P, Bai FQ, Lin DW, Peng HP, Hu Y, Zheng YJ, et al. One-pot green synthesis of mussel-inspired myoglobin-gold nanoparticles-polydopamine-graphene polymeric bionanocomposite for biosensor application. J Electroanal Chem. 2016;764:104–9. https://doi.org/10.1016/j.jelechem.2016.01.020.
66. Zhu Y, Lu S, Manohari AG, Dong X, Chen F, Xu W, et al. Polydopamine interconnected graphene quantum dots and gold nanoparticles for enzymeless H_2O_2 detection. J Electroanal Chem. 2017;796:75–81. https://doi.org/10.1016/j.jelechem.2017.04.017.
67. Loget G, Wood JB, Cho K, Halpern AR, Corn RM. Electrodeposition of polydopamine thin films for DNA patterning and microarrays. Anal Chem. 2013;85(21):9991–5. https://doi.org/10.1021/ac4022743.
68. Wan Y, Zhang D, Wang Y, Qi P, Hou B. Direct immobilisation of antibodies on a bioinspired architecture as a sensing platform. Biosens Bioelectron. 2011;26(5):2595–600. https://doi.org/10.1016/j.bios.2010.11.013.
69. Wang L, Miao L, Yang H, Yu J, Xie Y, Xu L, et al. A novel nanoenzyme based on Fe_3O_4 nanoparticles@thionine-imprinted polydopamine for electrochemical biosensing. Sensors Actuators B Chem. 2017;253:108–14. https://doi.org/10.1016/j.snb.2017.06.132.
70. Łuczak T. Preparation and characterization of the dopamine film electrochemically deposited on a gold template and its applications for dopamine sensing in aqueous solution. Electrochim Acta. 2008;53(19):5725–31. https://doi.org/10.1016/j.electacta.2008.03.052.
71. Vatrál J, Boča R, Linert W. Oxidation properties of dopamine at and near physiological conditions. Monatsh Chem. 2015;146(11):1799–805. https://doi.org/10.1007/s00706-015-1560-2.
72. Kanyong P, Rawlinson S, Davis J. Fabrication and electrochemical characterization of polydopamine redox polymer modified screen-printed carbon electrode for the detection of guanine. Sensors Actuators B Chem. 2016;233:528–34. https://doi.org/10.1016/j.snb.2016.04.099.
73. Zangmeister RA, Morris TA, Tarlov MJ. Characterization of polydopamine thin films deposited at short times by autoxidation of dopamine. Langmuir. 2013;29(27):8619–28. https://doi.org/10.1021/la400587j.
74. Elgrishi N, Rountree KJ, McCarthy BD, Rountree ES, Eisenhart TT, Dempsey JL. A practical beginner's guide to cyclic voltammetry. J Chem Educ. 2018;95(2):197–206. https://doi.org/10.1021/acs.jchemed.7b00361.
75. Voccia D, Sosnowska M, Bettazzi F, Roscigno G, Fratini E, De Franciscis V, et al. Direct determination of small RNAs using a biotinylated polythiophene impedimetric genosensor. Biosens Bioelectron. 2017;87:1012–9. https://doi.org/10.1016/j.bios.2016.09.058.
76. Vernitskaya TYV, Efimov ON. Polypyrrole: a conducting polymer; its synthesis, properties and applications. Russ Chem Rev. 1997;66(5):443–57. https://doi.org/10.1070/RC1997v066n05ABEH000261.
77. Sapurina I, Riede A, Stejskal J. In-situ polymerized polyaniline films: 3. Film formation. Synth Met. 2001;123(3):503–7. https://doi.org/10.1016/S0379-6779(01)00349-6.
78. MacDiarmid AG. "Synthetic metals": a novel role for organic polymers (Nobel lecture). Angew Chem Int Ed. 2001;40(14):2581–90.
79. Zhou Y, Yin H, Sui C, Wang Y, Ai S. Photoelectrochemical detection of 5-hydroxymethylcytosine in genomic DNA based on M. HhaI methyltransferase catalytic covalent bonding. Chem Eng J. 2019;357:94–102. https://doi.org/10.1016/j.cej.2018.09.138.

80. Yu Y, Huang Z, Zhou Y. Facile and highly sensitive photoelectrochemical biosensing platform based on hierarchical architectured polydopamine/tungsten oxide nanocomposite film. Biosens Bioelectron. 2019;126:1–6. https://doi.org/10.1016/j.bios.2018.10.026.
81. Bettazzi F, Laschi S, Voccia D, Gellini C, Pietraperzia G, Falciola L, et al. Ascorbic acid-sensitized Au nanorods-functionalized nanostructured TiO_2 transparent electrodes for photoelectrochemical genosensing. Electrochim Acta. 2018;276:389–98. https://doi.org/10.1016/j.electacta.2018.04.146.
82. Li J, Li X, Zhao Q, Jiang Z, Tadé M, Wang S, et al. Polydopamine-assisted decoration of TiO_2 nanotube arrays with enzyme to construct a novel photoelectrochemical sensing platform. Sensors Actuators B Chem. 2018;255:133–9. https://doi.org/10.1016/j.snb.2017.06.168.
83. Bettazzi F, Palchetti I. Photoelectrochemical genosensors for the determination of nucleic acid cancer biomarkers. Curr Opin Electrochem. 2018;12:51–9. https://doi.org/10.1016/j.coelec.2018.07.001.
84. Wang R, Ma H, Zhang Y, Wang Q, Yang Z, Du B, et al. Photoelectrochemical sensitive detection of insulin based on CdS/polydopamine co-sensitized WO_3 nanorod and signal amplification of carbon nanotubes@polydopamine. Biosens Bioelectron. 2017;96:345–50. https://doi.org/10.1016/j.bios.2017.05.029.
85. Çakıroğlu B, Özacar M. A self-powered photoelectrochemical glucose biosensor based on supercapacitor Co_3O_4-CNT hybrid on TiO_2. Biosens Bioelectron. 2018;119:34–41. https://doi.org/10.1016/j.bios.2018.07.049.
86. Son EJ, Kim JH, Kim K, Park CB. Quinone and its derivatives for energy harvesting and storage materials. J Mater Chem A. 2016;4(29):11179–202. https://doi.org/10.1039/c6ta03123d.
87. Nam HJ, Kim B, Ko MJ, Jin M, Kim JM, Jung DY. A new mussel-inspired polydopamine sensitizer for dye-sensitized solar cells: controlled synthesis and charge transfer. Chem Eur J. 2012;18(44):14000–7. https://doi.org/10.1002/chem.201202283.
88. Feng J, Li F, Li X, Wang Y, Fan D, Du B, et al. Label-free photoelectrochemical immunosensor for NT-proBNP detection based on La-CdS/3D $ZnIn_2S_4$/Au@ZnO sensitization structure. Biosens Bioelectron. 2018;117:773–80. https://doi.org/10.1016/j.bios.2018.07.015.
89. Karakouz T, Holder D, Goomanovsky M, Vaskevich A, Rubinstein I. Morphology and refractive index sensitivity of gold island films. Chem Mater. 2009;24(21):5875–85. https://doi.org/10.1021/cm902676d.
90. Tesler AB, Chuntonov L, Karakouz T, Bendikov TA, Haran G, Vaskevich A, et al. Tunable localized plasmon transducers prepared by thermal dewetting of percolated evaporated gold films. J Phys Chem C. 2011;115:24642–52. https://doi.org/10.1021/jp209114j.